ISSN 2616-5767 Vol.9, Issue 1: 72-79, DOI: 10.25236/AJETS.2026.090109

Terahertz Detection Mechanisms and HEMT Modeling for GaN-Based Receivers

Bo Lyu[1,*], Yuhang Liu[2]

[1]*FAE Group, Shenzhen CECport Technologies Co., Ltd, Shanghai, China*
[2]*IC Research and Design Department, Suzhou Link-IC Co., Ltd., Shanghai, China*
[*]*Corresponding author*

Abstract: *First, this project developed a simple High Electron Mobility Transistor (HEMT) model in AWR software and evaluated its operation as a detector at a low frequency of 10 GHz. The project then analyzed the results to explain why plasma resonance, rather than electron migration, is used for terahertz radiation detection. Secondly, the current-voltage (I-V) characteristics of the HEMT, along with a recurrence of the self-mixing model for verification, were used to establish the relationship between the detector and the signal. A responsivity scan was conducted for the AC response analysis results, and suggestions for further work on this project were provided. This project also performed a noise analysis of the Noise Equivalent Power (NEP) and examined AC responses under terahertz interaction, illustrating differences among models. Finally, the project validated a commercial HEMT model as a control group and defined key parameters of terahertz detectors to lay the foundation for subsequent antenna integration.*

Keywords: *Terahertz detection; GaN HEMT; Plasma resonance; Self-mixing model; Noise Equivalent Power*

1. Introduction

Fleming [1] first coined the term "terahertz" in 1974, when it was associated with the well-known concept of the "terahertz gap" in radio sounding. "The Gap" (Fig. 1) refers to the lack of adequate terahertz radiation detection techniques. The limitation caused by lost bandwidth hinders the development of communication technologies. As computer science advances in accordance with Moore's Law, the amount of wireless information transmission will eventually reach a physical limit related to electron behavior. Since the breakthrough in terahertz science and technology several decades ago, multiple technologies have helped overcome the "terahertz divide" [2]. In this project, electromagnetic radiation is treated as being composed of photons; thus, the term "light" in this thesis refers to electromagnetic radiation of any frequency.

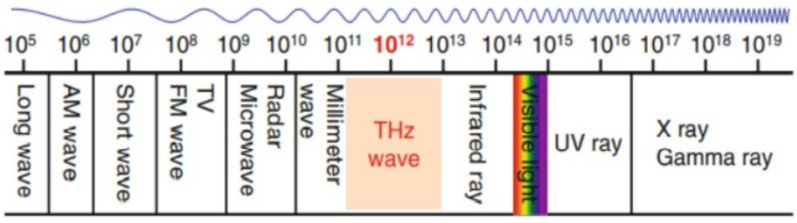

Fig. 1 THz region spectrum

The study of terahertz systems is likely to be a hot topic in the evolution of communication technologies. Currently, the main wireless communication methods used in daily life are based on Quadrature Amplitude Modulation (QAM), whether in 4G, 5G, or Wi-Fi systems. A single code expression in QAM is given by:

$$s_k(t)=A_k \cos(\omega_0 t+\theta_k), \quad kT<t\leq(k+1)T$$

while Multiple Quadrature Amplitude Modulation (MQAM) is expressed as:

$$s_{MQAM}(t)=\sum_n A_n g(t-nT_s)\cos(\omega_c t+\varphi_n)$$

ISSN 2616-5767 Vol.9, Issue 1: 72-79, DOI: 10.25236/AJETS.2026.090109

Here, (A_n) represents the amplitude range of the fundamental signal, $(T_s)$is the width of a single fundamental signal waveform, and $(g(t-nT_s))$denotes the waveform function. The expression for MQAM can be transformed into:

$$s_{MQAM}(t)=\left[\sum_n X_n\, g(t-nT_s)\right]\cos(\omega_c t)-\left[\sum_n Y_n\, g(t-nT_s)\right]\sin(\omega_c t)$$

The amount of information carried in the waveform increases as more signals are incorporated; however, the error rate also increases with the number of signals carried. If the frequency of the carrier wave is increased, the error rate issue can be alleviated because the time consumed by a single signal transmission is reduced. Another advantage of exploring higher frequencies is the availability of larger bandwidth, which allows more parallel signals to be transmitted simultaneously.

The detection of terahertz radiation is accompanied by changes in physical properties [4]; some techniques quantify the changes caused by thermal effects of terahertz radiation [5]. Another technical approach to measuring terahertz radiation involves monitoring electronic transitions induced by terahertz radiation [3]. Specifically, high electron mobility transistors (HEMTs) can be used to create a two-dimensional electron gas (2DEG), which can interact with terahertz radiation. Cooled bolometers and cooled photoconductors exhibit optimal performance at low temperatures, making them suitable choices for astronomical applications. Nevertheless, at room temperature [6], electronic detectors demonstrate better detection capabilities than thermal detectors. In recent years, terahertz detection based on plasma waves has been applied to modeling, and the simulation of high-sensitivity detectors also provides a favorable opportunity for the use of 2DEGs created by AlGaN/GaN heterostructures [7]. Therefore, research on gallium nitride (GaN) HEMT terahertz receivers will fill a gap in radio detection for the entire communication system.

2. Terahertz Detection Mechanism

2.1. Figure of Merit

Responsivity is defined as the ratio of the average output electrical signal (either voltage drop or current) to the average input power signal (incident terahertz radiation power).

It is expressed as voltage responsivity:

$$(R_{V/W}=\frac{V}{P})$$

Or current responsivity:

$$(R_{A/W}=\frac{I}{P})$$

Numerous publications on HEMT research propose different equations for defining responsivity; thus, in this thesis, a general equation:

$$(R=\frac{\eta q}{h\nu})$$

is used to evaluate the responsivity of the detector. In this equation, (q)represents the induced charge, $(h\nu)$denotes the energy of the terahertz wave (where (h) is Planck's constant and (ν) is the frequency of the terahertz wave), and (η) is the efficiency factor used to assess responsivity.

2.2. Noise Equivalent Power

Noise Equivalent Power (NEP) is a fundamental measure of detector sensitivity: the smaller the NEP value, the higher the detector sensitivity. However, it is important to note that different authors use NEP in different ways [8]. As the name suggests, the unit of NEP should be watts, and some authors express NEP values in watts. A parameter related to NEP is the detectivity (D^*). For a detector with area (A) and spectral bandwidth (Δf), the detectivity is given by:

$$D^*=\frac{\sqrt{A\Delta f}}{NEP}$$

ISSN 2616-5767 Vol.9, Issue 1: 72-79, DOI: 10.25236/AJETS.2026.090109

In this paper, the root mean square (RMS) value is used to describe the input terahertz wave power as an AC input, with the following relevant equations:

$$L=(2N\text{-}1)\frac{\lambda_p}{4},\quad \lambda_p=\frac{2\pi s}{\omega_p}$$

$$S=\sqrt{\frac{e(V_g\text{-}V_{th})}{m^*}}$$

where (N=1,2,3,…), (λ_p) is the plasma wavelength, (s) is the plasma wave speed, (e) is the electron charge, (V_g) is the gate voltage, (V_{th}) is the threshold voltage, and (m^*) is the effective electron mass.

2.3. Self-Mixing with Plasmonic Effects

In the early 1990s, Dyakonov proposed that terahertz radiation induces collective vibrations of carriers in the form of plasma waves [9]. Correspondingly, plasmonic waves generate terahertz-induced DC photocurrents in the field-effect transistor (FET) channel, opening up a new avenue for room-temperature terahertz detection. This work was followed by the development of the classical hydrodynamic transport model, which explains the rectification of the two-dimensional electron gas (2DEG) through resistive self-mixing in transistor channels.

The frequency of the plasma mode in the 2DEG can be expressed as:

$$\omega_N=(2N\text{-}1)\omega_0$$

where ($\omega_0=\frac{\pi}{2L}\sqrt{\frac{e(V_g\text{-}V_{th})}{m^*}}$). Here, a field-effect channel defines a plasma cavity with a gate length (L); (N=1,2,3,…); (V_g) and (V_{th}) are the gate voltage and the threshold voltage at channel pinch-off, respectively; and the size of the cavity (L) and the electron density (related to (V_g)) determine the plasma mode.

For a simple plasma cavity, the plasma frequency is given by:

$$f_{mnp}=\frac{1}{2\sqrt{\varepsilon\mu}}\sqrt{\left(\frac{m}{L_1}\right)^2+\left(\frac{n}{L_2}\right)^2+\left(\frac{p}{L_3}\right)^2}$$

where (m,n,p=1,2,3,…), (ε) is the permittivity of the medium, and (μ) is the permeability of the medium. The lowest resonant frequency is:

$$f_{110}=\frac{1}{2\sqrt{\varepsilon\mu}}\sqrt{\left(\frac{1}{L_1}\right)^2+\left(\frac{1}{L_2}\right)^2}$$

Thus, when the plasma cavity is scaled to the nanometer size, it can be tuned to the terahertz frequency spectrum. Research by Dyakonov and Shur indicates that the 1/4-wavelength characteristic of the cavity is the optimal choice for terahertz detection. For terahertz detectors, when terahertz waves enter and excite resonant or non-resonant plasma waves in the field-effect channel, the electrons in the channel interact with the plasma waves to induce a current. The DC voltage detected by the receiver proposed in this paper characterizes the magnitude of this induced current, converting the amplitude of the terahertz wave into a proportional DC voltage drop.

3. Terahertz Receiver Modelling

To achieve terahertz detection, this project first defined the parameters of the detector. Key characteristics of terahertz detectors include frequency range, noise level, responsivity, linearity, response time, coherence, and polarization sensitivity. Since this project focuses on building a suitable model for the detector and its antenna, it begins with the validation of a commercial HEMT model as a control group. An advanced antenna model with an optimized structure was adopted to enhance terahertz wave detection. Finally, thermal and pulse detectors were used to evaluate the performance of the final-stage GaN detectors, as these detectors can detect broader broadband signals than other types [2].

ISSN 2616-5767 Vol.9, Issue 1: 72-79, DOI: 10.25236/AJETS.2026.090109

The commercial HEMT used in this paper is the CG2H40010F from Wolfspeed. By measuring the induced voltage of the device under its operating voltage, an ideal induced voltage curve was obtained. The performance and effectiveness of the receiver designed in this paper should be close to this ideal result. The test schematic and the simulation results are shown in Fig. 2. The device exhibits high current drive capability, with the drain-source voltage (V_{DS}) ranging from -2.5 V to 2.5 V; this clearly demonstrates the typical behavior of FETs in the linear region. According to the datasheet [10], the device operates normally at a threshold voltage ((V_{th}=-3 V)), which can be inferred from the saturation region (where (V_{DS}=10 V\) and (I_{DS}=3.6 mA)). In the saturation region, the drain-source current (I_{DS}) increases as the gate-source voltage (V_{GS}) increases.

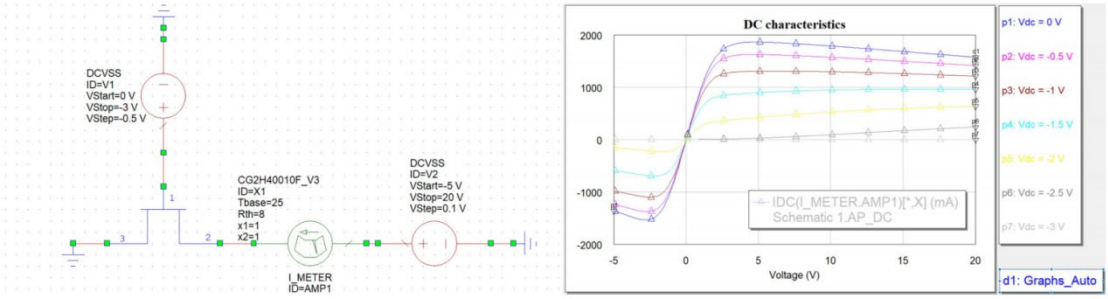

Fig. 2 Commercial HEMT testing schematic and results

4. HEMT Modeling for Terahertz Receivers

To achieve terahertz detection, this project first defined the parameters of the detector. Key characteristics of terahertz detectors include frequency range, noise level, responsivity, linearity, response time, coherence, and polarization sensitivity. Since this project focuses on building a suitable model for the detector, it begins with the validation of a commercial HEMT model as a control group. Finally, thermal and pulse detectors were used to evaluate the performance of the final-stage GaN detectors, as these detectors can detect broader broadband signals than other types.

The commercial HEMT used in this paper is the CG2H40010F from Wolfspeed. By measuring the induced voltage of the device under its operating voltage, an ideal induced voltage curve was obtained. The performance and effectiveness of the receiver designed in this paper should be close to this ideal result. The test schematic and the simulation results are shown in Fig. 2. The device exhibits high current drive capability, with the drain-source voltage V_{DS} ranging from -2.5 V to 2.5 V; this clearly demonstrates the typical behavior of FETs in the linear region. According to the datasheet, the device operates normally at a threshold voltage ($V_{th} = -3$ V), which can be inferred from the saturation region (where $V_{DS} = 10$ V and $I_{DS} = 3.6$ mA). In the saturation region, the drain-source current I_{DS} increases as the gate-source voltage V_{GS} increases.

5. Simulation Results Analysis

An important application of this project is the development of a wireless communication system with a data rate exceeding 10 Gb/s. Typically, a wireless communication system includes at least a transmit antenna and a receive antenna. A common formula used to calculate transmit power and receive power in a transmission system is the Friis transmission formula. In the Friis transmission formula [11]:

$$P_R = \frac{P_T G_T G_R \lambda^2}{(4\pi R)^2}$$

(G_T) represents the transmit antenna gain, (G_R) represents the receive antenna gain (note: the original text mentioned "receive antenna loss," which is corrected here to align with the Friis formula), (P_T) is the transmit power, (P_R) is the receive power, (λ) is the wavelength of the signal, and (R) is the distance between the transmit and receive antennas. From the Friis formula, it can be inferred that if the loss of the receive antenna is reduced, the received signal power increases. The main objective of developing the receive system is to improve the received power level and the detector's responsivity, while maintaining satisfactory speed and noise levels.

By analyzing the radio frequency (RF) response of the HEMT, the simulation model can deduce the main operating frequency range of the plasma. The device will exhibit optimal performance when the

ISSN 2616-5767 Vol.9, Issue 1: 72-79, DOI: 10.25236/AJETS.2026.090109

antenna resonates with the eigenfrequency of the plasma. However, due to the simplification of physical equations, the calculations may not be as accurate as the performance of actual devices; thus, multiple computer simulations and parameter corrections were also considered. Another challenge in performance optimization is the trade-off between different characteristics: some improvements in responsivity may increase costs. For example, the use of asymmetric antennas increases both cost and chip area.

In this paper, the butterfly antenna was selected as the final designed structure; the S-parameters model of the antenna was exported as a data file and imported into AWR for circuit simulation. The resulting circuit diagram is shown in Fig. 3.

The HEMT model used in this circuit diagram is the advanced Angelov HEMT model, and its equivalent circuit diagram is shown below. The advanced Angelov model provides a single entry point for multiple versions of the well-known Angelov/Zirath/Rorsman (or Chalmers) model and its derived versions (Fig. 4).

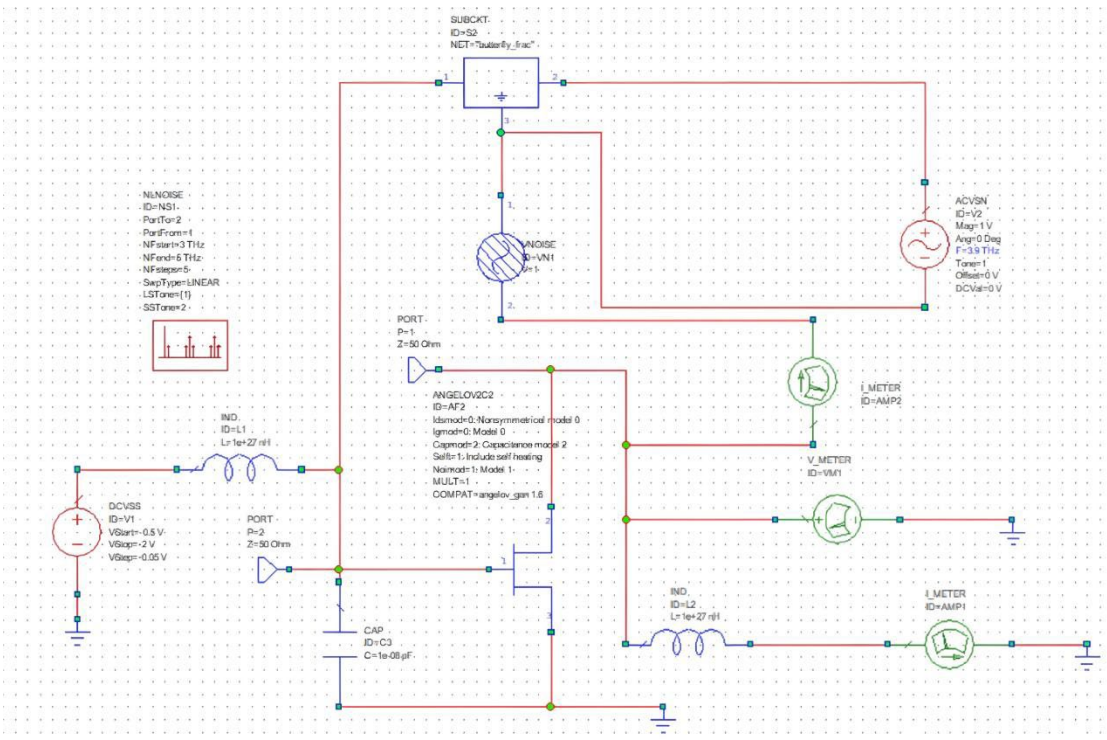

Fig. 3 Schematic using to simulate the responsivity and NEP

AWR currently supports four different versions of this model. The original version corresponds to the Chalmers model, with all recent updates focusing on supporting GaN FETs [10]. The second and third versions are implementations of the Angelov model for ADS (Advanced Design System), as described in the equations provided in the ADS documentation. The third version of the model (Fig. 5) is an improvement over the second version, incorporating additional modifications to enhance compatibility with the ADS model version.

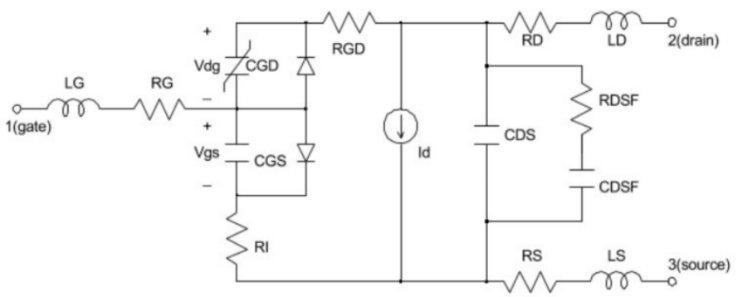

Fig. 4 Original version of angelov model – Chalmers model

ISSN 2616-5767 Vol.9, Issue 1: 72-79, DOI: 10.25236/AJETS.2026.090109

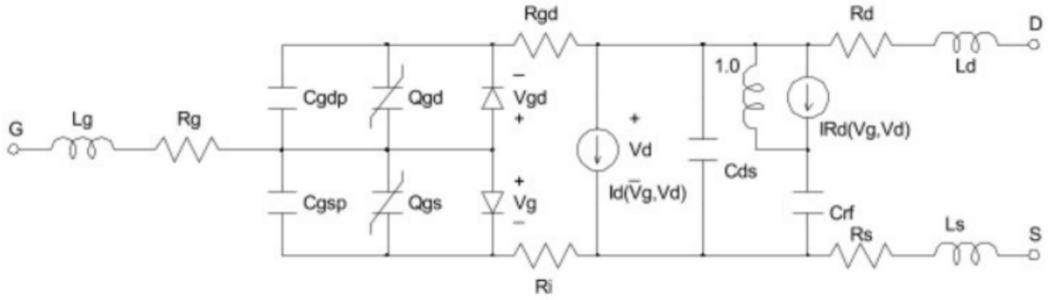

Fig. 5 Third version of angelov model

5.1. Responsivity

In this experiment, the input AC signal current was varied. Due to antenna attenuation, the voltage of the terahertz wave entering the HEMT source changed with the AC current. The source voltage waveforms under different currents are shown in Fig. 6. Different bias voltages generate 2DEG resonators of different sizes; the DC voltages generated by resonating with different input terahertz waves are also shown in Fig. 6. The response waveform was derived using the relevant formula, as shown in Fig. 7. At 3.9 THz, the responsivity ranges from (10^3) to (1.5×10^4) V/W (or A/W, depending on the type of responsivity). This result is consistent with the findings of a study on room-temperature GaN terahertz detectors[11].

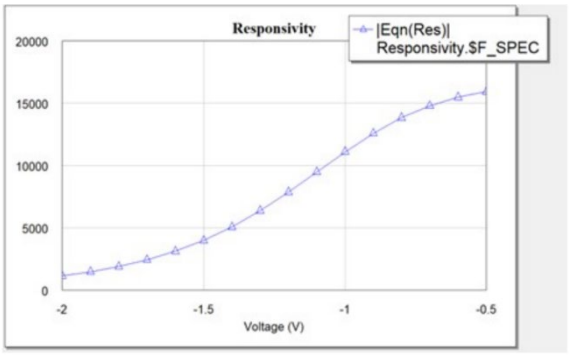

Fig. 6 Calculated Responsivity under bias from 0.5V to 2V

5.2. Noise Equivalent Power

The noise equivalent power (NEP) was calculated using the root mean square equation:

$$V_{RMS}=\sqrt{\frac{1}{T_2-T_1}\int_{T_1}^{T_2}[f(t)]^2dt}$$

At a given modulation frequency, wavelength, and effective noise bandwidth, the radiant power produces a signal-to-noise ratio (SNR) per unit power at the output of the detector.

In this case, the unit power is 2.4; thus, the NEP ranges from (1×10^{-9}) to $(4\times10^{-9}\ W/\sqrt{Hz})$ at 3.9 THz, as shown in Fig. 7.

ISSN 2616-5767 Vol.9, Issue 1: 72-79, DOI: 10.25236/AJETS.2026.090109

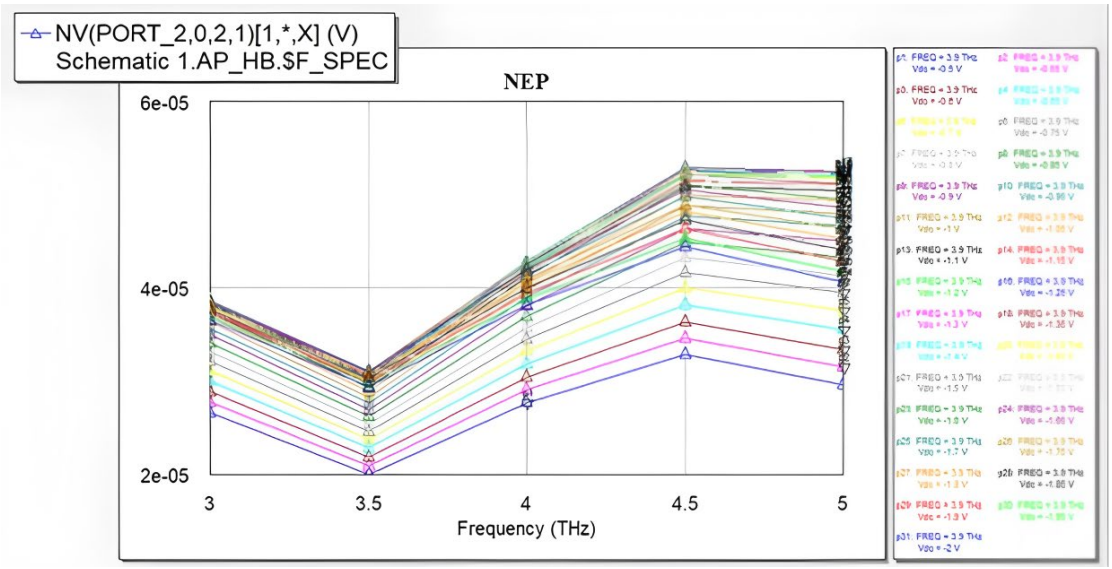

Fig. 7 Calculated NEP from 0.5V to 2V

6. Conclusions

Using the advanced Angelov HEMT model, the design results are in good agreement with predictions from a review of terahertz detectors, indicating that this device is suitable for engineering applications.

The main disadvantage of the current terahertz receiver is the small magnitude of the induced current. Since the required size of the 2DEG sensing cavity is on the nano-meter scale, the bias voltage must be controlled at a small amplitude. As a result, the source's input amplitude is prone to saturation, and the induced-voltage amplitude is correspondingly small as shown in Fig. 8. Currently, the resonant cavity operates at the zero point of resonance divergence; as the bias voltage decreases, the cross-sectional area of the 2DEG induction cavity decreases as well, thereby reducing the dissipation of resonant waves. However, if the bias voltage is too small, the induced voltage becomes excessively small—causing the noise of the amplifier circuit to affect the noise immunity of the entire system when the voltage is amplified.

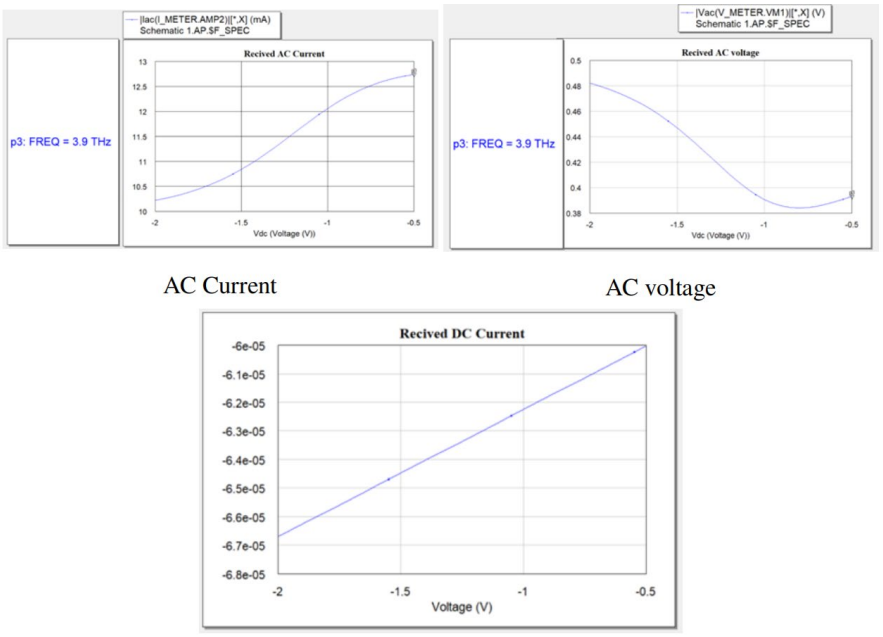

Fig. 8 Input AC and voltage and indicted DC voltage

ISSN 2616-5767 Vol.9, Issue 1: 72-79, DOI: 10.25236/AJETS.2026.090109

Acknowledgements

I would like to thank Professor Martin Cryan. His course on Advanced Optical Device Design provided directional guidance and ideas for this design. Additionally, as my supervisor, he offered guidance on academic matters, life, and future development throughout my master's studies, which reinforced my belief in pursuing further learning. At the same time, I wish to express my gratitude to Dr. Zhang Yutian for his meticulous guidance. As the initiator of the project idea, Dr. Zhang Yutian shared numerous antenna design concepts with me during our communications—concepts that were indispensable for completing this design.

References

[1] P. Siegel, "Terahertz technology," IEEE Transactions on Microwave Theory and Techniques, vol.50, no. 3, pp. 910–928, Mar. 2002, doi:10.1109/22.989974.
[2] R. A. Lewis, "A review of terahertz detectors," Journal of Physics D: Applied Physics, vol. 52, no.43, Oct. 23, 2019, doi:10.1088/1361-6463/ab31d5.
[3] "Terahertz gap," https://en.wikipedia.org/wiki/Terahertz_gap, accessed on September 10,2022.
[4] M. Sakowicz, M. B. Lifshits, O. A. Klimenko, et al., "Terahertz responsivity of field effect transistorsversus their static channel conductivity and loading effects," Journal of Applied Physics, vol. 110,no. 5, Sep. 1, 2011, doi:10.1063/1.3632058.
[5] P. Richards, "Bolometers for infrared and millimeter waves," Journal of Applied Physics, vol. 76,no. 1, Jul. 1, 1994, pp. 1–24, doi:10.1063/1.357128.
[6] F. Sizov and A. Rogalski, "THz detectors," Progress in Quantum Electronics, vol. 34, no. 5, Sep.2010, pp. 278–347, doi:10.1016/j.pquantelec.2010.06.002.
[7] X.-G. He, D.-G. Zhao, and D.-S. Jiang, "Formation of two-dimensional electron gas at AlGaN/GaNheterostructure and the derivation of its sheet density expression," Chinese Physics B, vol. 24, no.6, Jun. 2015, p. 067301, doi:10.1088/1674-1056/24/6/067301.
[8] X. Wang, Z. Pan, and C. Glennie, "A novel noise filtering model for photon-counting laser al-timeter data," IEEE Geoscience and Remote Sensing Letters, vol. 13, no. 7, 2016, pp. 947–951,doi:10.1109/LGRS.2016.2555308.
[9] M. Dyakonov and M. Shur, "Detection, mixing, and frequency multiplication of terahertz radiationby two-dimensional electronic fluid," IEEE Transactions on Electron Devices, vol. 43, no. 3, 1996,pp. 380–387, doi:10.1109/16.485650.
[10] Y. Wen, W. Ma, J. Bailey, G. Matmon, and X. Yu, "Broadband terahertz metamaterial absorberbased on asymmetric resonators with perfect absorption," IEEE Transactions on Terahertz Scienceand Technology, vol. 5, no. 3, May 2015, pp. 406–411, doi:10.1109/TTHZ.2015.2401392.
[11] "The Friis equation," https://www.antenna-theory.com/basics/friis.php, accessed onSeptember 10, 2022.